

PHOTODEGRADATION OF METHYLCYCLOHEXANE IN TWO PHASES WITH MODIFIED-TITANIA IMMOBILIZED ON PUMICE

Slamet^{1*}, Oktrianto², Agung Hendarsa¹, Ratnawati³, Salim Mustofa⁴

¹*Department of Chemical Engineering, Faculty of Engineering, Universitas Indonesia, Kampus UI Depok, Depok 16424, Indonesia*

²*Department of Chemical Engineering, Universitas Surya Bogor, Tangerang 15810, Indonesia*

³*Department of Chemical Engineering, Institut Teknologi Indonesia, Tangerang 15320, Indonesia*

⁴*National Nuclear Energy Agency (BATAN), Kawasan Puspitek, Tangerang 15320, Indonesia*

(Received: March 2016 / Revised: November 2016 / Accepted: January 2017)

ABSTRACT

The photocatalytic degradation of methylcyclohexane (MCH) in two phases (aqueous and vapor) was examined using modified titania that was immobilized on pumice and performed in the system of a specific condition. The photodegradation system that used a particular configuration reactor and modified catalyst could facilitate the two-phase photodegradation of MCH simultaneously. The photocatalyst was prepared by the mechanical mixing of urea and TiO₂ P25 with mass ratios of 1:3 and 2:3, respectively and then calcined at 350 and 450°C. This modified photocatalyst was then immobilized on pumice and finally used for the photodegradation of MCH. The Infrared spectra studies revealed that modified titania with urea successfully incorporated a non-metal dopant within the TiO₂ lattice. The catalyst that spread evenly across the surface of the pumice can be seen from Scanning Electron Microscope (SEM) characterization. The loading of 7.5% mass photocatalyst that immobilized on pumice degraded MCH in two-phases simultaneously during a 120 minute period and can be considered the optimum condition.

Keywords: Methylcyclohexane; Modified-titania; Photodegradation; Pumice

1. INTRODUCTION

Volatile organic compounds (VOCs) are known to have long-term effects on human health (United States Environmental Protection Agency, US EPA, 1991), to affect stratospheric ozone depletion processes (Wiederkehr, 1994), to affect the photochemical formation of tropospheric ozone (ground-level) in the presence of nitrogen oxides (Atkinson et al., 1985), and to contribute to the greenhouse effect (Balaji & Murugesan, 2010). One of the VOCs is methylcyclohexane (MCH). It is a constituent of different fuels (Spain & Somerville, 1985), used in paint diluents (Kim et al., 2011), in organic synthesis (Campbell, 1987), and as solvents for cellulose ethers (US EPA, 1991). MCH can also be found in urban atmospheres with a range of 0.2–0.8 ppbv (Hernandez-Alonso et al., 2011). In this paper, MCH is considered a liquid waste that is found in some oil wells that contain MCH at high concentrations.

MCH at a high level should be considered volatile and it occurs in two distinct phases that can be dissolved in water with a small amount up to 14 ppm at 25°C (US EPA, 1991). Hernández-Alonso et al. (2011) reported on the photocatalytic oxidation of MCH in a vapor phase using

*Corresponding author's email: slamet@che.ui.ac.id, Tel. +62-21-7863516, Fax. +62-21-7863515
Permalink/DOI: <https://doi.org/10.14716/ijtech.v8i1.3337>

TiO₂, whereas Hamdy et al. (2012) reported on it in a liquid phase. They successfully degraded MCH. Thus, to facilitate the photodegradation of MCH in two-phases, a reactor with a particular configuration is required. This study focused on the degradation of MCH in two-phases simultaneously, namely the vapor phase and the liquid phase, as this remains substantially missing in the work of some researchers.

Advanced oxidation processes (AOPs), such as the photocatalysis process or plasma technology, are efficient novel methods used to accelerate non-selective oxidation, and thus, the destruction of a wide range of resistant organic substances has occurred. A report on MCH photodegradation was mentioned earlier. Currently, the most widely used photocatalyst is TiO₂ because it presents a relatively high level of photoactivity and is stable, inexpensive, and innocuous (Ratnawati et al., 2015). Unfortunately, the use of TiO₂ is limited due to its high band-gap energy ($E_g = 3.2$ eV), which requires ultraviolet (UV) light irradiation for its photocatalytic activity. In contrast, the UV light of the sun accounts for only a small fraction (3–5%) of the sun's light spectrum compared to visible light (Wang et al., 2011).

Currently, the photocatalyst application on the site poses a disadvantage due to the difficulty of infiltration for eliminating particles and recycling the catalyst. Filtration can be reduced by immobilizing the photocatalyst on a solid support, such as quartz, silica, glass, ceramics, activated carbon, zeolites, and pumice (Rao et al., 2003). In addition, the immobilization of the catalyst on pumice can make the catalyst float on the liquid surface so that the photocatalyst, photon, and pollutant in the aqueous and vapor phases will be in one condition simultaneously. The last advantage of using a two-phase reactor for MCH degradation is that it is soluble in water in small concentrations.

In this study, we investigated the photodegradation of MCH in the aqueous and vapor phases simultaneously with modified titania immobilized on pumice. The modified photocatalyst was prepared by the dry mixing of TiO₂ P25 with urea and was immobilized on pumice to facilitate MCH degradation in the two-phases. The catalyst that was immobilized on pumice acted as a floating device that could be applied to degrade MCH outdoors with sunlight exposure and to eliminate the filtration processes of the catalyst. All MCH photocatalytic degradation was carried out in an entirely closed reactor to prevent evaporation, and therefore the photodegradation of MCH in the two-phases could occur simultaneously.

2. EXPERIMENTAL

2.1. Materials

Commercial powder of TiO₂ P25 (79% anatase, 21% rutile, specific surface area SSA of 50±15 g.m⁻²) was obtained from Evonik Industries. Urea from Dabang (Chemical formula: CH₄N₂O, MW: 60.06 g.mol⁻¹, purity: 94%) was used as the C and N precursors. Methylcyclohexane (chemical formula: C₆H₁₁CH₃, MW: 98,19 g. mol⁻¹, assay ≥ 99%) was provided by Merck. Tetra ethyl ortho silicate (TEOS – chemical formula: Si(OC₂H₅)₄, MW: 208 g.mol⁻¹, purity 98%) was provided by Sigma Aldrich. Natural pumice was supplied from Bima City, Nusa Tenggara Barat, Indonesia.

2.2. Preparation of C–N Co-doped TiO₂

One gram of urea (dopant source for N and C) was crushed until it became a powder, added into 3 g of TiO₂ P25, and dry mixed for 5 minutes. The mixture was then calcined in an atmospheric furnace at 350°C for 2 hours. Subsequently, the sample was cooled to room temperature, and the washing process was continued. The sample was dipped in a 0.1N hydrochloric acid solution and sonicated for 30 minutes to break the TiO₂ aggregates. Then, the sample was filtrated with 2.5µm of a cellulose membrane filter to separate with its suspended. Next, the

sample was re-heated in the atmospheric furnace at 350°C for 1 hour, cooled down to room temperature, and finally sieved with 45 μm of mesh.

TiO₂ P25 photocatalyst were prepared through a mixing process with urea at various urea:P25 mass ratios (1:3 and 2:3), calcined at 350°C for 2 hours, and denoted as CN-TiO₂-350 and 2CN-TiO₂-350, respectively. For the urea: P25 mass ratio of the 1:3 sample, calcination at a temperature of 450°C for 2 hours was also performed (denoted as CN-TiO₂-450). The last treatment was done to study the effect of temperature on the decomposition of urea that allows the dopant of N and C to be incorporated into the TiO₂ lattice.

2.3. Catalyst Characterization

The surface elemental composition was characterized using the INSPECT-F50 Field Emission Scanning Electron Microscope (FE-SEM) equipped with energy dispersive X-ray spectroscopy (EDX). The infrared spectra were obtained using a Shimadzu IR Prestige-21 FTIR and were recorded as a potassium bromine (KBr) disc (1:10 sample/KBr) over a wavenumber range of 400–4000 cm^{-1} . Raman spectra were obtained in a SENTERRA Dispersive Raman Microscope that used an Ar laser (785 nm) with an intensity of 10 mW for excitation. X-ray diffraction (XRD) patterns were measured on a Shimadzu XD-610 diffractometer with Cu K α radiation ($\lambda=0.154$ nm) over the 2θ range of 20–80°. The scan rate used for XRD analysis was set to 2°/min, whereas the accelerating voltage was 40 kV at an applied current of 40 mA. The UV–vis diffuse reflectance spectra (DRS) were recorded at room temperature between 200 and 800 nm using a Shimadzu UV2450 spectrophotometer.

2.4. Photocatalytic Activity Measurement

The photocatalytic degradation of MCH was performed on a particular system that combined a configuration reactor and modified catalyst. This fully closed pyrex reactor has a volume of 1.2 liters and consists of a photocatalyst immobilized on pumice, on a magnetic stir bar, and in MCH. The photodegradation process used a high-pressure mercury lamp a Philips HPL-N (250W) as a photon source featuring approximately 83% of visible light and the rest UV light (Slamet *et al.*, 2013).

Modified photocatalyst immobilized TiO₂ on pumice with a dimension of 4–6 mm (denoted as PS) was set in various loading using a dip coating method. The photocatalyst CN-TiO₂-350 and pumice were placed in a solution of TEOS (0.23 vol%) as the silica source (denoted as CN-TiO₂-350/PS).

The photodegradation of MCH began with 60 $\mu\text{mol/L}$ as the initial concentration that was injected into the reactor containing 30 g of the catalyst CN-TiO₂-350/PS and 500 mL of deionized water. Degradation was started at room temperature, at 28°C, and stirred for 60 minutes without the irradiation of photons to allow the system to reach an adsorption-desorption equilibrium. Then, an analysis of samples was drawn from the reactor every 30 minutes during all of the processes. The concentration of MCH was analyzed by gas chromatography with a flame ionization detector (GC-FID Shimadzu 2014, 250°C) using a 30m length of the capillary column.

3. RESULTS AND DISCUSSION

3.1. FE-SEM/EDX

Figure 1 shows the FE-SEM images for PS and CN-TiO₂-350/PS samples. This characteristic clearly shows that the CN-TiO₂-350 photocatalyst closed the surface of pumice. Elemental compositions of modified TiO₂ are summarized in Table 1, which indicates that besides Ti and O, the elements of N and C were detected on CN-TiO₂-350. The elemental composition of CN-TiO₂-350/PS showed that the CN-TiO₂-350 photocatalyst had been immobilized on pumice

because the elemental composition on CN-TiO₂-350/PS consisted of Si, Al, Ca, Na, Fe, and K.

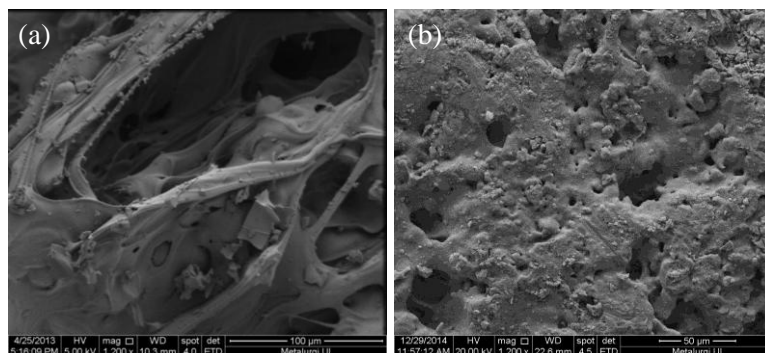


Figure 1 SEM images with magnification of 1200x for (a) pumice; (b) CN-TiO₂-350/PS

Table 1 EDX Results for P25, CN-TiO₂, and Pumice (PS)

Element	% Mass			
	P25	CN-TiO ₂ -350	CN-TiO ₂ -450	CN-TiO ₂ -350/PS
Ti	58.61	50.77	49.79	15.93
O	41.39	33.48	41.32	52.65
N	-	7.28	1.24	9.13
C	-	8.47	7.65	14.17
Si	-	-	-	4.29
Al	-	-	-	1.42
Ca	-	-	-	0.24
Na	-	-	-	1.19
Fe	-	-	-	0.63
K	-	-	-	0.35

The selected range of temperatures used in this study (350 and 450°C) did not significantly affect the C content of the products. The probable reason for this observation was due to the relatively low-temperature usage during the sample calcination. On the other hand, the amount of N seems to be reduced with increasing calcination temperatures. This phenomenon was also reported by Sato et al. (2005).

3.2. FTIR Spectroscopy

The fourier transform infrared (FTIR) spectra of P25 and C-N co-doped TiO₂ prepared with urea and a calcination temperature of 350°C are shown in Figure 2. The absorption band at 1630 cm⁻¹ is assigned to the bending vibration of surface hydroxyl (surface-adsorbed water molecules). The peak at around 1719 cm⁻¹ is attributed to the presence of carbonate species, whereas the peak at 1427 cm⁻¹ was observed for the C-N co-doped TiO₂ samples. Meanwhile, a very weak absorption peak at 1050 cm⁻¹ is assigned to the N-Ti-O stretching vibration. This similar observation was reported by Ratnawati et al. (2014). The formation of C-N co-doped TiO₂ (C-N-Ti) and N-Ti-O indicated successful N-doping through the replacement of the oxygen atoms in TiO₂. This result is supported by the Raman spectra result (Figure 3).

3.3. Raman Spectroscopy

Figure 3 shows the Raman spectra of the CN-TiO₂-350 and P25 samples. This result supported the FTIR characterization results demonstrating the existence of the elements of C and N, which has incorporated into TiO₂ lattice. The Raman peaks of the Ti-O-Ti network over a 300 - 800 cm⁻¹ range are characteristic features of anatase and rutile structures. Raman spectroscopy analysis reveals the presence of bands at 396, 514, and 636 cm⁻¹, attributed to the B_{1g}, A_{1g} + B_{1g}

and E_g anatase active modes (Yang et al., 2010). The peak at 447 cm^{-1} indicates the presence of rutile and calcination treatment at 350°C , causing the amount of rutile to become more than that found in TiO_2 P25.

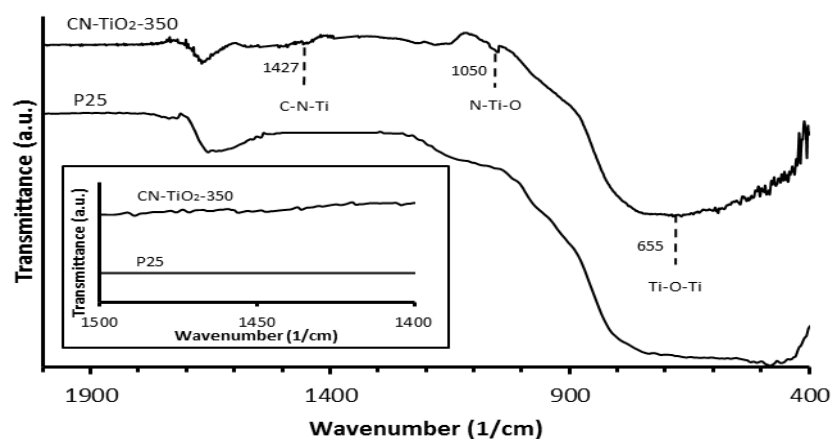


Figure 2 FTIR spectra of P25 and $\text{CN-TiO}_2\text{-350}$

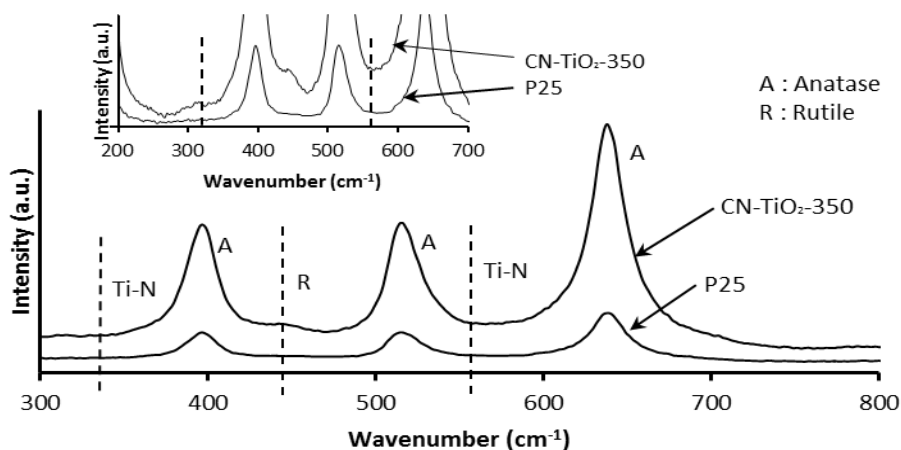


Figure 3 Raman spectra of P25 and $\text{CN-TiO}_2\text{-350}$

The Raman peaks of N-implanted particles became broader than those of the original TiO_2 (Figure 3). In the Raman spectra of the layers, the bands at 330 and 550 cm^{-1} are the first-order scattering of non-stoichiometric titanium nitride (Gyorgy et al., 2002). The low-frequency scattering at 330 cm^{-1} is caused by acoustical phonons, whereas at around 550 cm^{-1} , it is due to optical phonons. This result is in agreement with the FTIR result that indicated the presence of N in the TiO_2 lattice. According to Kiran and Sampath (2012), the peak of Ti-C would arise at the wavenumber 1078 cm^{-1} . However, in this experiment, this peak was not detected because C was not bonded to Ti; rather it bonded to N to form C-N co-doped TiO_2 (C-N-Ti) as previously reported in the FTIR analysis.

3.4. X-Ray Diffraction (XRD)

Figure 4 shows the XRD patterns for P25 and C-N- $\text{TiO}_2\text{-350}$. As Nawawi and Nawi (2014) observed, no phase transformation occurred for the calcined samples at 350°C . Using the Debye-Scherrer formula, the average crystalline size was found to be 20.23 nm and 21.29 nm for P25 and $\text{CN-TiO}_2\text{-350}$, respectively. It can be seen that characteristic peaks at $2\theta = 25.3^\circ$ (JCPDS no. 21-1272) and 27.4° (JCPDS no. 21-1276) corresponded to the anatase and rutile

phases, respectively. This result supports the Raman spectra where each sample consists of the anatase and rutile phases. Because C and N atoms were incorporated into the CN-TiO₂-350 lattice, the diffraction peaks were not detected, as those atoms were highly dispersed and had a small amount of content on CN-TiO₂-350 (Ratnawati et al., 2014).

3.5. UV – Vis DRS

Figure 5a shows the UV-Vis diffused reflectance spectra of P25 and CN-TiO₂-350 and Table 2 displays a reduction in their band gap. This phenomenon indicates that the elements of N and C have been incorporated into the TiO₂ lattice, and it is assumed that the mid-gap of the N 2p or N-O levels are located above the valence band of O 2p than a mixture of N 2p states and O 2p. These results were reported by Di Valentin et al. (2007), which predicted that substitutional and interstitial N would create the occupied N 2p and N-O states located at 0.14 eV and 0.73 eV above the O 2p valence band edge, respectively.

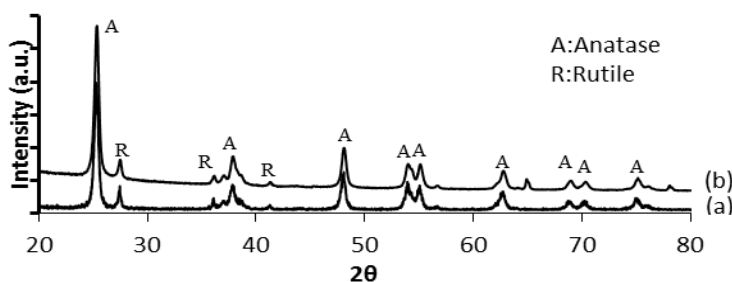


Figure 4 X-ray diffraction patterns for: (a) P25; and (b) CN-TiO₂-350

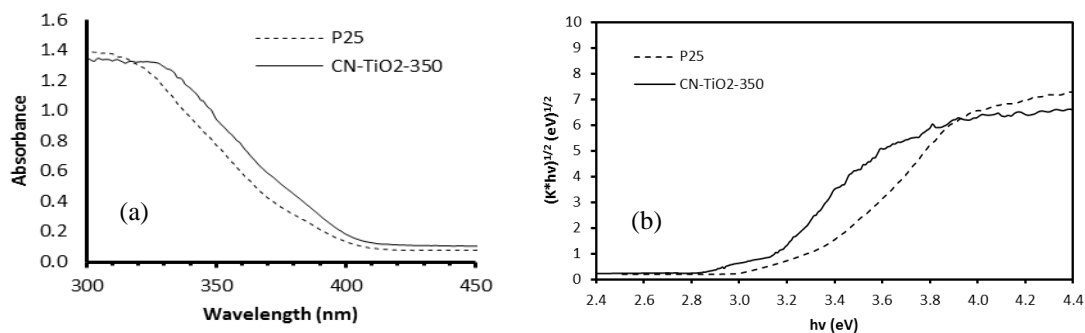


Figure 5 (a) UV-Vis diffused reflectance spectra of P25 and CN-TiO₂-350; and (b) plots of the transformed Kubelka-Munk

Table 2 Bandgap of titania P25 and CN co-doped TiO₂

Modified Photocatalyst	Bandgap, E _g (eV)
CN-TiO ₂ -350	3.05
2CN-TiO ₂ -350	2.95
CN-TiO ₂ -450	3.00
P25	3.25

Figure 5b shows an apparent reduction in the band gap energy for CN-TiO₂-350 (became 3.05 eV) compared to the reference of a typical band gap value for TiO₂ P25 (3.25 eV). Because CN-TiO₂-350 undergoes a reduction in the band-gap unlike TiO₂ P25, it might show enhanced photoresponse under visible light.

The increase of the N:TiO₂ ratio (2CN-TiO₂-350) has a greater effect on the visible light absorption of TiO₂ and leads to a monotonic increase in optical absorption (Yang et al., 2010). Meanwhile an increase in the calcination temperature (CN-TiO₂-450), which affects the band-gap, was also reported by Nawawi and Nawi (2014).

3.6. Photocatalytic Degradation of MCH

About 60 μmol/L of MCH in the aqueous and vapor phases was degraded by CN-TiO₂-350/PS, and it occurred simultaneously because the photocatalyst was floated on the water surface in the reactor. Figure 6 shows that 1.7 μmol/L of MCH was soluble in water and degraded simultaneously with MCH in the vapor phase, so that after 120 minutes, the conversion of the liquid phase and vapor phase was 100% and 64%, respectively. Gonzalez et al. (1999) reported a similar observation, where photodegradation occurred under UV light, yielding an 8.18% conversion of aqueous MCH. MCH was dissolved in the water in a small concentration so that it could be degraded 100% by catalyst CN-TiO₂-350/PS. The process was started with adsorption by the photocatalyst in the first 30 minutes before degradation when the light was on. For the MCH vapor, it may directly degrade when dissolved in water. When the MCH in the liquid phase is already degraded, the MCH vapor will dissolve in the liquid phase continuously until the equilibrium absorption of MCH by water is achieved. Hamdy et al. (2012) predicted that the photocatalytic oxidation of MCH in the liquid phase would generate carboxylate and carbonate species before entirely converted into CO₂ and H₂O.

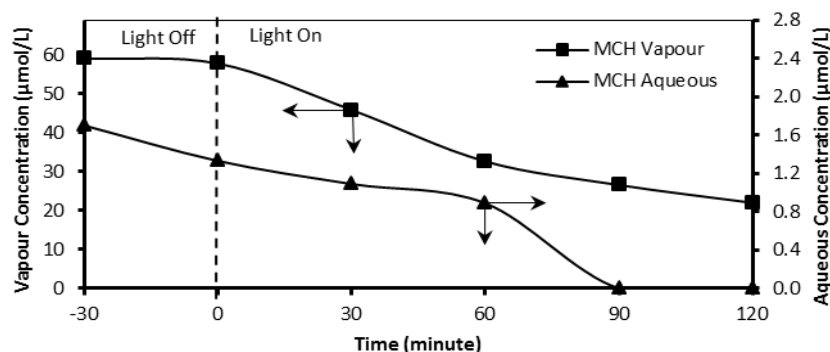


Figure 6 Photodegradation of MCH in aqueous and vapor phases simultaneously with CN-TiO₂-350/PS

Figure 6 depicts that the initial concentration of MCH was more dominant in the vapor phase, that is, 35 times more than that dissolved in water. Therefore, the next study will focus on the degradation of MCH in the vapor phase. The photodegradation of MCH vapor with CN-TiO₂-350/PS was better than that with P25/PS, achieving a result of by 55% reduction. Liu et al. (2007) reported a similar observation, where the photocatalytic activity of MCH occurred under UV light. This phenomenon proved that decreasing the band-gap energy in the CN-TiO₂-350/PS had an impact on improving the photocatalytic activity in the degradation of MCH. However the reduction was not maximized, caused by the degradation process's being carried out in a closed reactor, thereby limiting the amount of oxygen involved. Martinez et al. (2011) conducted previous research on reactive species of oxygen deficiency due to the fact that sufficient moisture in the air inhibits NO photocatalytic degradation at high pollutant concentrations.

Figure 7 shows that the CN-TiO₂-450/PS catalyst has lower photocatalytic activity than does CN-TiO₂-350/PS in the degradation of MCH, even when it is compared to P25/PS. This finding is possible because, according to the EDX result, the amount of N seems to be reduced with increasing calcination temperatures. Sato et al. (2005) reported a similar observation. They indicated that the element of N was not stable when bonded to Ti-O, allowing for

decomposition along with increasing temperature. It was also observed that the addition of urea into double (2CN-TiO₂-350/PS) would also reduce the photocatalytic efficiency of the modified photocatalyst because CN-TiO₂-350/PS degraded better than 2CN-TiO₂-350/PS did. On the one hand, the N that was incorporated into the TiO₂ lattice could result in the band-gap's narrowing and the red-shift of the absorption edge toward the visible light region that increased its photocatalytic activity. However, when the N content is higher than the optimum amount, it could form a large recombination center that eventually reduces its photocatalytic activity (Nawawi & Nawi, 2014).

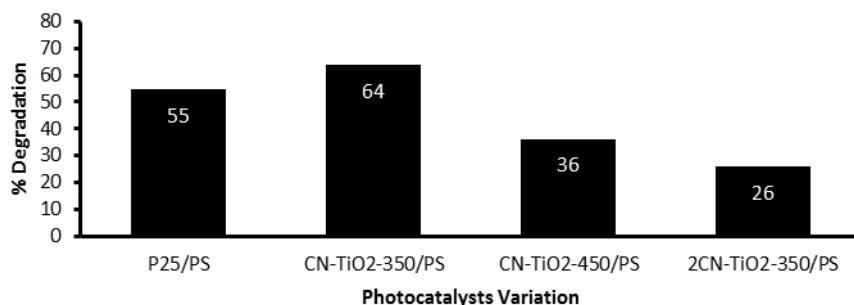


Figure 7 Photodegradation of MCH vapor with various types of catalysts after 120 minutes at initial concentration of 60 $\mu\text{mol/L}$

Because the photocatalyst CN-TiO₂-350/PS gave the best performance for degrading MCH, this photocatalyst was used to study the effect of the CN-TiO₂-350 loading variation (0%, 2.5%, 5%, 7.5%, and 10%) on pumice. Figure 8a shows that MCH was degraded for 120 minutes, and its conclusion can be seen in Figure 8b. The initial concentration of the MCH vapor about – 60 $\mu\text{mol/L}$ – is denoted as C_0 , and the ratio of the residual concentration to the initial concentration is denoted as C/C_0 . Pumice with a loading of 0% of CN-TiO₂-350 eliminated MCH by about 4%. This condition indicated that the elimination process occurred due to MCH adsorption by pumice. Increasing the percentage of the loading CN-TiO₂-350 indicated that more MCH was degraded, as a greater catalyst amount increases the active surface area of the photocatalyst.

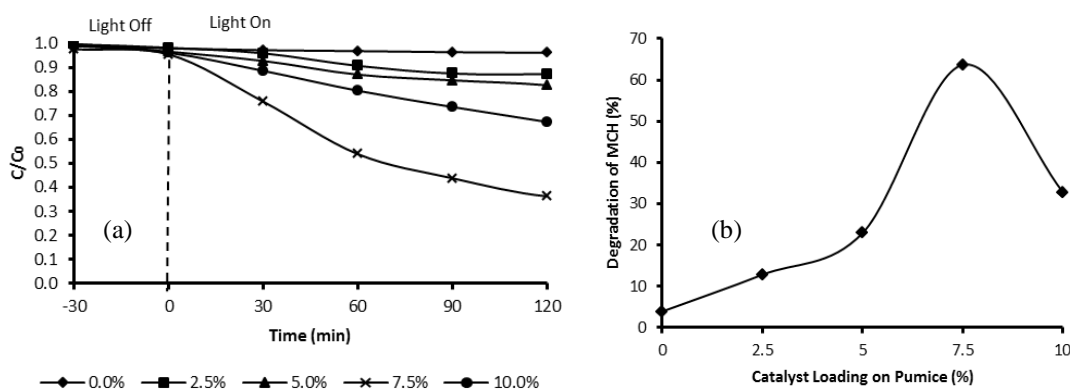


Figure 8 Effect of CN-TiO₂-350 loading on pumice: (a) changes in concentration; and (b) percentage of MCH photodegradation ($t = 120$ min)

The loading of CN-TiO₂-350 from 0% to 10% reaches the maximum photocatalytic activity at a 7.5% loading of CN-TiO₂-350 on pumice (Figure 8b). Increasing the catalyst loading exceeds the optimum loading, causing the pores of pumice to be closed by the catalyst and therefore increasing the density of the composite. This reduces the ability of pumice as an adsorbent and

as a floating media of catalyst support. In addition, Figure 1 shows that the pores of pumice are closed by the photocatalyst.

4. CONCLUSION

The photocatalytic degradation of MCH in the aqueous and vapor phases occurred simultaneously with a catalyst immobilized on pumice. The optimum condition of pumice with a 7.5% modified catalyst that used a 3:1 P25:urea mass ratio and was calcined at 350°C (CN-TiO₂-350/PS) was used for the degradation of MCH. After 120 minutes of degradation, the conversion of each liquid phase and vapor phase was 100% and 64%, respectively. In this study, MCH looks much more dominant in the vapor phase. Under our experimental conditions, MCH vapor was eliminated by 64% on CN-TiO₂-350/PS, whereas it was eliminated by 55% on P25/PS during a 120-minutes period.

5. ACKNOWLEDGEMENT

The authors would like to thank the Directorate General of Higher Education, Indonesian Ministry of National Education (DIKTI) for the financial support for this research (MP3EI 2014), and the National Nuclear Energy Agency of Indonesia (BATAN) for providing Raman spectroscopy TiO₂ characteristics and XRD measurements.

6. REFERENCES

- Atkinson, R., 1985. Kinetics and Mechanism of the Gas-Phase Reactions of Hydroxyl Radical with Organic Compounds under Atmospheric Conditions. *Chemical Reviews*, Volume 85, pp. 69–201
- Balaji, S., Murugesan, A.G., 2010. Assessment of Volatile Organic Compound (VOC) Emissions from a Petrochemical Industry in Ranipet, South India. *Journal of Environmental Research and Development*, Volume 4(4), pp. 939–946
- Campbell, M.L., 1987. *Cyclohexane*. In: Ullman's Encyclopedia of Industrial Chemistry, Volume A8, pp. 209–215, VCH Publishers, New York
- Di Valentin, C., Finazzi, E., Pacchioni, G., Selloni, A., Livraghi, S., Paganini, M.C., Giamello, E., 2007. N-Doped TiO₂: Theory and Experiment. *Chemical Physics*, Volume 339, pp. 44–56
- Gonzalez, M.A., Howell, S.G., Sikdar, S.K., 1999. Photocatalytic Selective Oxidation of Hydrocarbons in the Aqueous Phase. *Journal of Catalysis*, Volume 183, pp. 159–162
- Gyorgy, E., Perez del Pino, A., Serra, P., Morenza, J.L., 2002. Surface Nitridation of Titanium by Pulsed Nd:YAG Laser Irradiation. *Applied Surface Science*, Volume 186, pp. 130–134
- Hamdy, M.S., Amrollahi, R., Mul, G., 2012. Surface Ti³⁺ Containing (Blue) Titania: A Unique Photocatalyst with High Activity and Selectivity in Visible Light-Stimulated Selective Oxidation. *ACS Catalysis*, Volume 2, pp. 2641–2647
- Hernandez-Alonso, M.D., Tejedor-Tejedor, I., Coronado, J.M., Anderson, M.A., 2011. Operando FTIR Study of the Photocatalytic Oxidation of Methylcyclohexane and Toluene in Air over TiO₂-ZrO₂ Thin Films. *Applied Catalysis B: Environmental*, Volume 101, pp. 283–293
- Kim, H.Y.; Kang, M.G.; Kim, T.G.; Kang, C.W., 2011. Effect of Methylcyclohexane on the Reproductive System of SD Rats. *Safety and Health at Work*, Volume 2, pp. 290–300
- Kiran, V., Sampath, S., 2012. Enhanced Raman Spectroscopy of Molecules Adsorbed on Carbon-Doped TiO₂ Obtained from Titanium Carbide. *ACS Applied Materials and Interfaces*, Volume 4, pp. 3818–3828

- Liu, W., Gao, J., Zhang, F., Zhang, G., 2007. Preparation of TiO₂ Nanotubes and Their Photocatalytic Properties in Degradation Methylcyclohexane. *Materials Transactions*, Volume 48(9), pp. 2464–2466
- Martinez, T., Bertron, A., Ringot, E., Escadeillas, G., 2011. Degradation of NO using Photocatalytic Coatings Applied to Different Substrates. *Building and Environment*, Volume 46(9), pp. 1808–1816
- Nawawi, W.I., Nawi, M.A., 2014. Carbon Coated Nitrogen Doped P25 for the Photocatalytic Removal of Organic Pollutants under Solar and Low Energy Visible Light Irradiations. *Journal of Molecular Catalysis A: Chemical*, Volume 383–384, pp. 83–93
- Rao, K.V.S., Rachel, A., Subrahmanyam, M., Boule, P., 2003. Immobilization of TiO₂ on Pumice Stone for the Photocatalytic Degradation of Dyes and Dye Industry Pollutants. *Applied Catalysis B: Environmental*, Volume 46, pp. 77–85
- Ratnawati, Gunlazuardi, J., Dewi, E.L., Slamet, 2014. Effect of NaBF₄ Addition on the Anodic Synthesis of TiO₂ Nanotube Arrays Photocatalyst for Production of Hydrogen from Glycerol-Water Solution, *International Journal of Hydrogen Energy*, Volume 39, pp. 16927–16935
- Ratnawati, Gunlazuardi, J., Slamet., 2015. Development of Titania Nanotube Arrays: The Roles of Water Content and Annealing Atmosphere. *Material Chemistry and Physics*, Volume 160, pp. 111–118
- Sato, S., Nakamura, R., Abe, S., 2005, Visible-Light Sensitization of TiO₂ Photocatalysts by Wet-Method N Doping. *Applied Catalysis B: Environmental*, Volume 284(1-2), pp. 131–137
- Slamet, Tristantini, D., Valentina, Ibadurrohman, M., 2013. Photocatalytic Hydrogen Production from Glycerol–Water Mixture over Pt-N-TiO₂ Nanotube Photocatalyst. *International Journal of Energy Research*, Volume 37(11), pp. 1372–1381
- Spain, J.C. and Somerville, C.C., 1985, Fate and Toxicity of High Density Missile Fuels RJ-5 and JP-9 in Aquatic Test Systems. *Chemosphere*, Volume 14, pp. 239–248
- United States Environmental Protection Agency (US EPA), 1991. *Health and Environmental Effect Document for Methylcyclohexane*. Office of Health and Environmental Assessment, Cincinnati, OH, USA
- Wang, P., Zhou, T., Wang, R., Lim, T.T., 2011. Carbon-Sensitized and Nitrogen-Doped TiO₂ for Photocatalytic Degradation of Sulfanilamide under Visible-Light Irradiation. *Water Research*, Volume 45, pp. 5015–5026
- Wiederkehr, P., 1994. Characterization and Control of Odours and VOC in the Process Industries 1st ed., *Elsevier Science*, Volume 61, pp. 11–28
- Yang, G., Jiang, Z., Shi, H., Xiao, T., Yan, Z., 2010. Preparation of Highly Visible-Light Active N-Doped TiO₂ Photocatalyst. *Journal of Materials Chemistry*, Volume 20, pp. 5301–5309